Life Sciences 228 (2019) 198–207

Contents lists available at ScienceDirect

Life Sciences

journal homepage: www.elsevier.com/locate/lifescie

Blocking CXCR3 with AMG487 ameliorates the blood-retinal barrier disruption in diabetic mice through anti-oxidative

Honggang Wang[a,1], Jianmei Li[a,1], Peiyu Zhong[a], Shuaiwei Wang[a], Lei Zhang[a], Ruisheng Yang[b], Dongdong Wu[a], Mingliang Chen[a], Ailing Ji[a,*], Yanzhang Li[a,*], Jun Wang[a,*]

[a] Henan University School of Basic Medical Sciences, Kaifeng 475004, China
[b] The First Affiliated Hospital of Henan University, Kaifeng, Henan 475001, China

ARTICLE INFO

Keywords:
CXCR3
Oxidative stress
Diabetic retinopathy
Blood-retinal barrier

ABSTRACT

Oxidative stress and blood-retinal barrier (BRB) damage induced by hyperglycemia are the principal processes involved in the early stages of diabetic retinopathy (DR). CXC chemokine receptor 3 (CXCR3)-mediated inflammatory infiltration exists in many disease models. The main objective of the present study was to determine whether AMG487, a CXCR3 antagonist, can ameliorate BRB disruption and reactive oxygen species generation in the DR model. The retinal endothelial cell and ganglion cell ultrastructures were observed using a transmission electron microscope. The pericyte marker PDGFR-β, tight junction occludin, and leaking albumin were evaluated. The oxidative stress level, CCAAT-enhancer-binding protein homologous protein (CHOP), and p-p38 expression were also investigated in vivo and in vitro. The results indicated that AMG487 application might alleviate PDGFR-β and occludin loss, and decreased the residual content of retinal albumin in the streptozocin-induced DR mouse model via the inhibition of oxidative and endoplasmic reticulum stress, in which p38 activation was also involved. Thus, CXCR3 inhibition might be a target to prevent the early stage of DR injury.

1. Introduction

Diabetic retinopathy (DR), the main leading cause of visual loss worldwide, is a chronic inflammatory disease that is triggered by hyperglycemia, and develops with the invasion of inflammatory cells and cytokines, and eventually leads to vessel degeneration and neuronal cell injury [1,2]. The hypoxia/ischemia, oxidative damage, pericyte loss, and endothelial apoptosis induced by hyperglycemia moves through the DR pathological process [3–6]. The blood-retinal barrier (BRB) breakdown is an early primary pathological event [1,7], which is attributed to the release of excessive cytokines, increasing leukostasis, and permeability of capillary vessels [8–10].

The family of CXC chemokines and their receptors play important roles in the regulation of vascular endothelial function and angiogenesis. CXC chemokine receptor 3 (CXCR3) and its ligand are members of the CXC chemokine family. CXCR3 was recognized initially as a receptor guiding T cell of directional migration [11]. Previous studies have shown that CXCR3 was expressed not only in macrophage/microglia, but also in endothelial cells and neurons [12–15]. Gene knockout of CXCR3 promoted the neuronal survival in an entorhinal cortex injury model by decreasing microglia recruitment [16]. Experiments in organotypic hippocampal slice cultures demonstrated that in CXCL10- and CXCR3-deficient mouse, the neuronal cell death in CA1 and CA3 regions decreased after *N*-methyl-D-aspartate (NMDA) application via a decrease of microglia accumulation [14]. CXCR3 activation in endothelial cells might prevent angiogenesis, and thus, compromise vascular integrity [12,13]. A recent study revealed that the CXCL10/CXCR3 pathway was mediated by endoplasmic reticulum (ER) stress, and participated in the retinal inflammation and injury in a high intraocular pressure mouse model [17]. Another study using an optic nerve crushed mouse model also showed that the CXCL10/CXCR3 axis played an important role in recruiting leukocytes and inducing retinal neuronal cell death [18]. DR has a similar pathological process, especially in retinal damage induced by inflammation and oxidative stress. However, there is limited information regarding the relationship between the progress of DR and the CXCR3 axis. A previous study reported that chemokine and CXCR3 were highly expressed in proliferative DR. Therefore, CXCR3 and CXCL10 might participate in the pathogenesis of DR [19]. To date, AMG487, a CXCR3 antagonist, is the only small molecule that has entered clinical trials and it has been

* Corresponding authors at: Henan University School of Medicine, JinMing Avenue, Northern Segment, Kaifeng, Henan 475004, China.
E-mail addresses: ailingji@163.com (A. Ji), yanzhang206@163.com (Y. Li), whb21c@vip.henu.edu.cn (J. Wang).
[1] Co-first author.

https://doi.org/10.1016/j.lfs.2019.04.016
Received 29 January 2019; Received in revised form 4 April 2019; Accepted 5 April 2019
Available online 27 April 2019

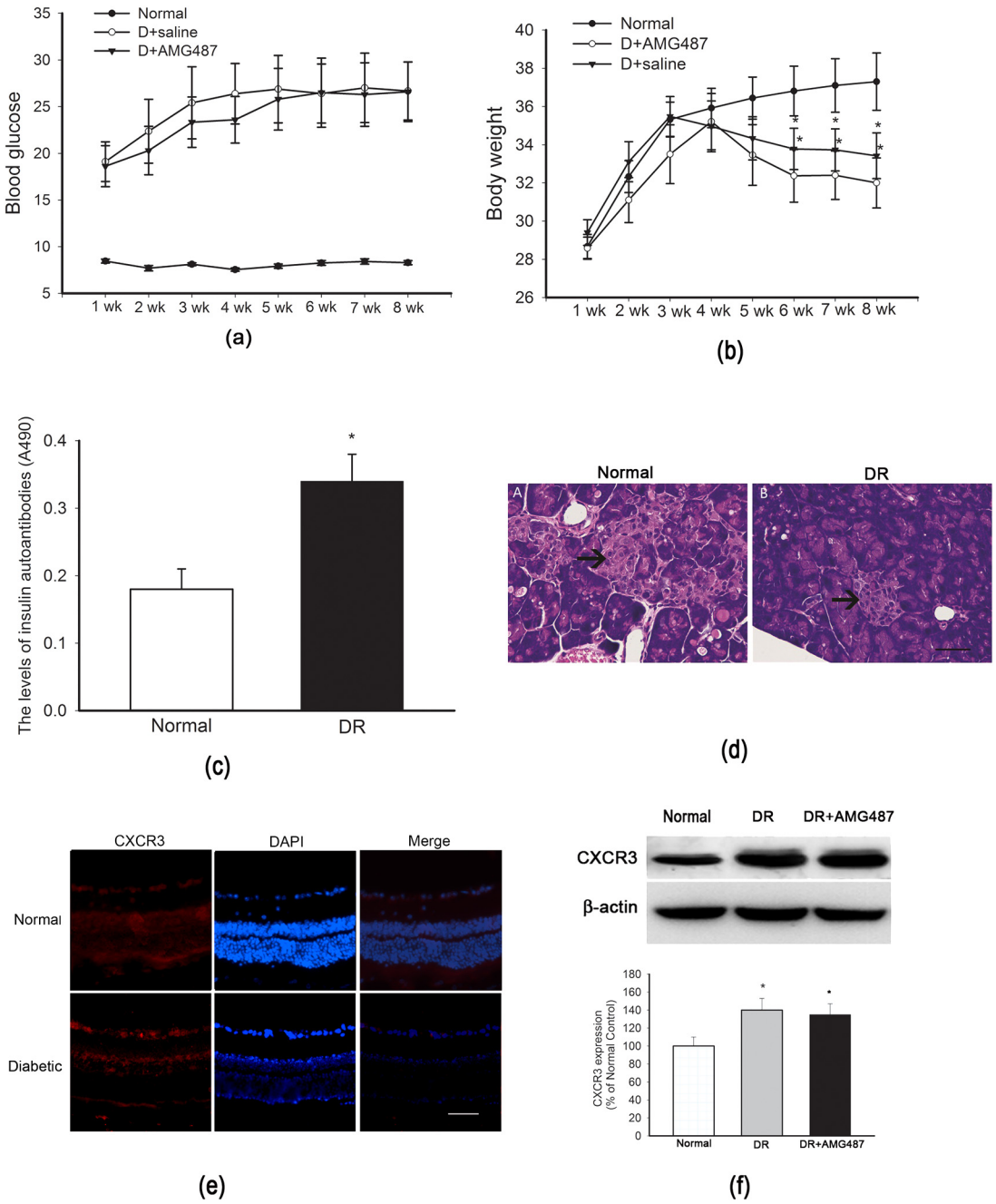

Fig. 1. General description of the animal model: The blood glucose level (a) and body weight (b) among normal, diabetic, and diabetic + AMG487 animals; the serum insulin autoantibody level was significantly higher in the STZ injection animals than in the control group animals (c); representative pancrease tissue slices with small pancrease islets and lower number of cells in STZ-induced diabetic group. Arrows indicate pancrease islets. (d); the expression of CXCR3 in normal, diabetic, and diabetic + AMG487 retinas. Representative images of immunohistochemical staining (e) and western blot analysis (f). D, diabetic. *P < 0.05, compared with the normal control group (Scale bar = 50 μm).

demonstrated to have efficacy in many pathological process [18,20,21]. Determining whether the CXCL10/CXCR3 axis influences BRB function during the early stage of DR, and what role it plays in the pathological process of oxidative stress and/or ER stress are the principal objectives of the present study.

2. Materials and methods

2.1. Animals

C57BL/6 male mice (8 weeks old) were obtained from the Model Animal Research Center of Nanjing University, and maintained in individual ventilation cages (IVC) cages (temperature 22 ± 2 °C; humidity 50%–60%), under a 12 h light/ 12 h dark cycle. Standard mouse food and tap water were provided ad libitum. The animal experiments were approved by the Committee of Medical Ethics and Welfare for experimental animals at the Henan University School of Medicine. Mice were anesthetized with pentobarbital (120 mg/kg) by intraperitoneal (i.p.) injection. The surgery complied with the committee's guidelines and efforts were made to minimize suffering.

2.2. Diabetic mouse model and treatment

The experimental diabetic mouse model was created in accordance

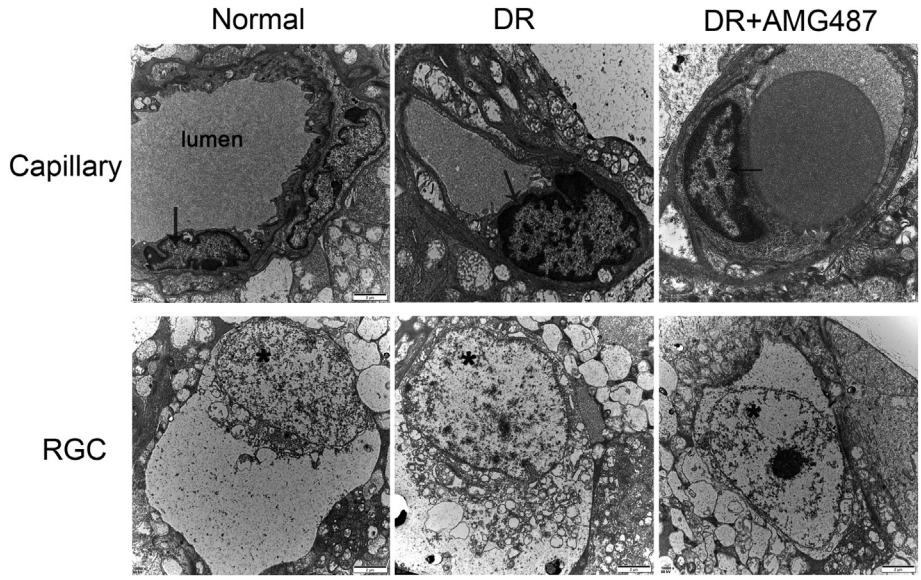

Fig. 2. Representative transmission electron microscopic images of capillary endothelial cells and retinal ganglion cell. Arrows indicate the endothelial cell nucleus. Asterisks indicate the retinal ganglion cell nucleus.

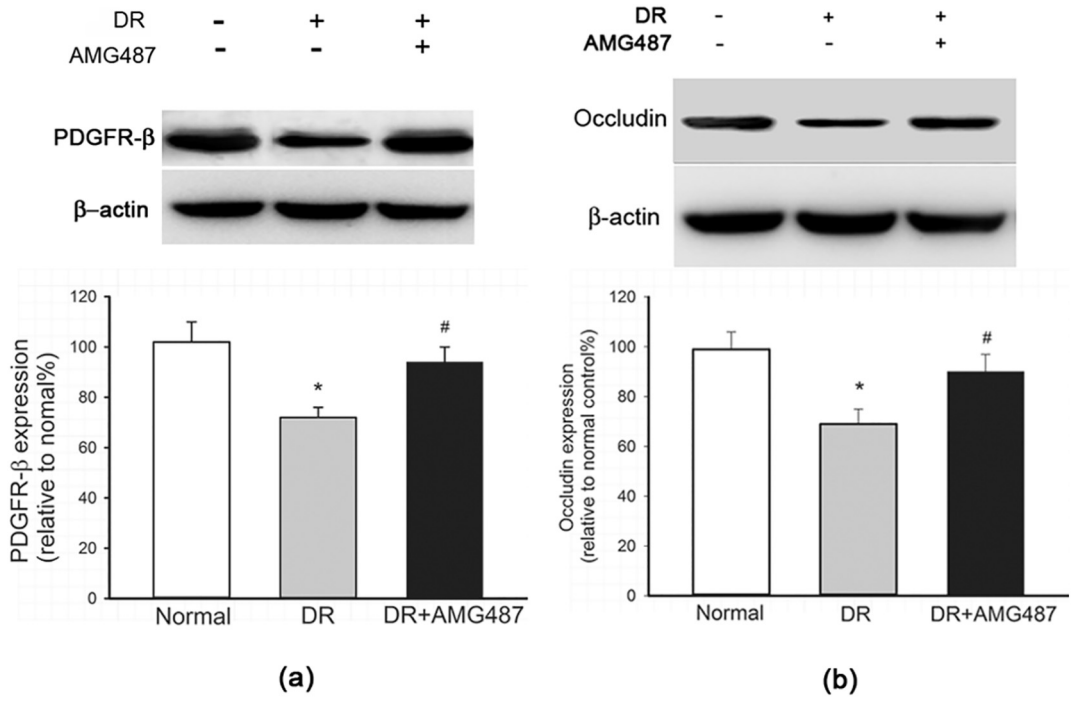

Fig. 3. AMG487 inhibited the decrease of PDGFR-β and occludin expression in DR retinas. Western blot analysis for the PDGFR-β and occludin expression indicated that AMG487 inhibited the decrease of PDGFR-β and occludin in diabetic group. *P < 0.05, compared with normal control group; #P < 0.05, compared with DR group.

with previous studies [22,23]. Animals were injected (i. p.) three times with 75 mg/kg Streptozotocin (STZ) (in 100 mM citrate buffer, pH 4.5) or only citrate buffer. The interval time between each injection was 24 h. Animals with blood glucose levels higher than 16 mmol/L were recognized as having diabetes within 1 week following STZ injection. The serum insulin antibody test (enzyme-linked immunosorbent assay, ELISA) and islet histology observation were performed to determine the type of diabetic model. Four weeks after STZ injection, animals were treated with AMG487 (5 mg/kg, subcutaneous injetion; *DR + AMG487 group*) or with dimethyl sulfoxide (*DR group*) for the following 4 weeks. The normal control group animals was not injected any drugs. The dose of AMG487 was chosen based on a previous experiment [24].

2.3. Preparation of electron microscope samples (transmission electron microscope, TEM)

The middle section of the retina was cut into small lumps (1 mm^3) and fixed in 2.5% glutaric dialdehyde for 2 h. After washing in phosphate buffered saline solution, the sample was placed in osmium tetroxide for post-fixation for 2 h. Then, the sample section (50–70 μm) was made after dehydration and embedding in epoxy resin. Localization was obtained under an optical microscope, after which the sample was stained with methylene blue. Ultrathin sections (1–2 μm) were made using an ultra-microtome (LKB-V, Sweden). After staining with uranyl acetate and lead citrate, images were observed and obtained using a

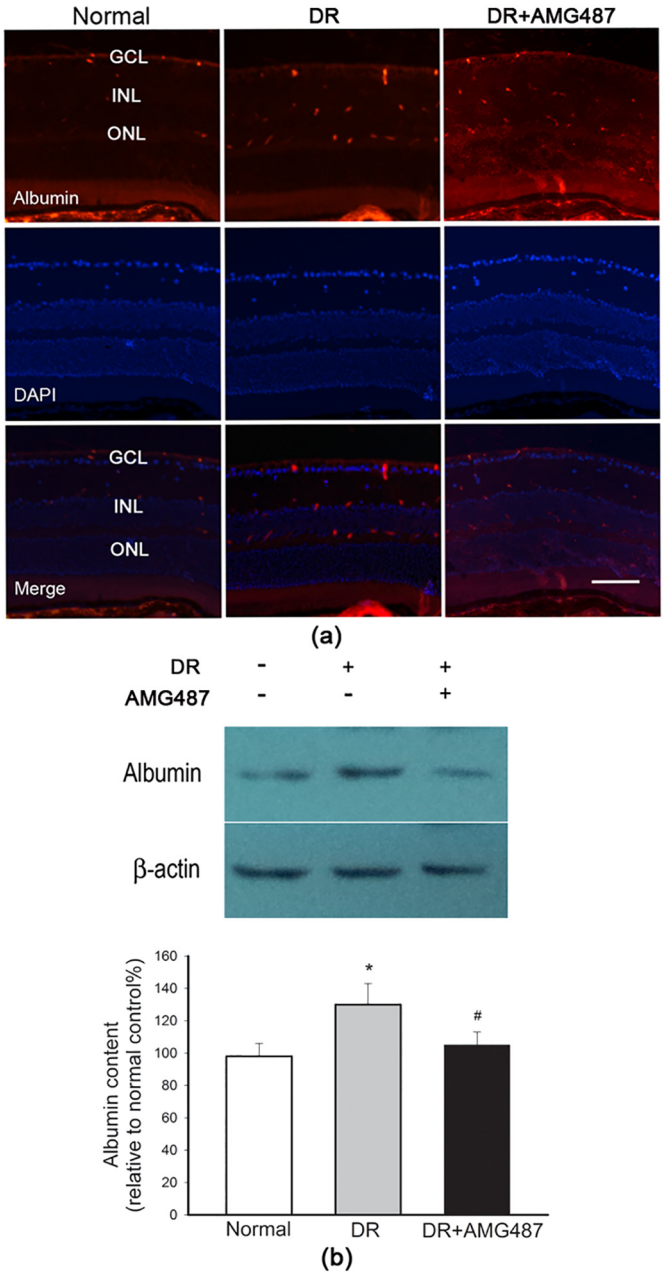

Fig. 4. AMG487 prevented the leaking albumin in DR retinas. (a) Immunohistochemical staining images, scale bar = 50 μm; (b) Western blot analysis shows the increased albumin in DR group were inhibited by the treatment of AMG487. GCL, ganglion cell layer; INL, inner nuclear layer; ONL, outer nuclear layer. *P < 0.05, compared with the normal control; #P < 0.05, compared with the DR group.

TEM-100SX (H-7650 HITACHI, Japan). Each group included 3–5 retinas in the observation.

2.4. Immunohistochemistry

The eyeballs were removed and fixed in 4% paraformaldehyde (4 °C) for 24 h. After dewaxing and antigen retrieval processes, the slides were blocked by 10% normal goat serum for 30 min, and then incubated overnight with the primary antibodies (PDGFR-β, Proteintech 1:500; occludin, Santacruz 1:200; albumin, Proteintech 1:300; an CCAAT-enhancer-binding protein homologous protein (CHOP), Beyotime Biotech 1:1000). The following day, after washing the sections three times with phosphate buffered saline solution, the sections were incubated in the appropriate secondary antibodies (Beyotime Biotech 1:500) for 1 h at room temperature (26 ± 3 °C). After washing, fluorescence images were obtained under a fluorescence microscope (Nikon Ti-E, Japan). Retinas from three animals were collected during this experiment.

For the cryosections, the eyeball was enucleated, embedded with Compound Tissue-Tek (SAKURA, USA), and fixed in liquid nitrogen. Retinal cryosections (5 μm) were incubated with Dihydroethidium (DHE) (40 min at room temperature). Image acquisition was completed under a fluorescence microscopy.

2.5. Western blotting analysis

After quickly isolating the retinas from the eyeballs and removing the pigmentary epithelium, retinal tissues were frozen in liquid nitrogen, and then placed in a − 80 °C refrigerator. Whole retinal tissues and HUVECs (Xinxiang medical university, China) were extracted in ice-cold radioimmunoprecipitation assay buffer (Beyotime Biotech, China). Each group included 4–6 retinas or samples. A total of 30 μg protein per sample was loaded onto each lane, separated by 10% SDS-PAGE, and then transferred onto the nitrocellulose membranes. After blocking in 3% BSA, the membranes were incubated with primary antibodies at 4 °C overnight (PDGFR-β, Proteintech 1:2000; occludin, Santacruz 1:500; albumin, Proteintech 1:1000; CHOP, Beyotime Biotech 1:2000; p38 and p-p38, Santacruz 1:400; and β-actin, CST 1:5000). The secondary antibody (horseradish peroxidase-conjugated) was incubated the next day. The blot bands were visualized using the electrochemiluminescence (ECL, Solarbio, China) technique. The optical densities were semi-quantified with Image J v2.1 analysis software. Beta-actin (β-actin) was used as a loading control.

2.6. Measurement of the extravasation albumin

After anesthesia, the animals were perfused with 37 °C phosphate-buffered saline solution for 5 min from the left ventricle to rinse out the blood cells and proteins. Then, western blot and immunostaining were performed to evaluate the vascular leakage by identifying the leaking albumin in the retinas. Four or five retinas per group were collected.

2.7. Cell culture

HUVECs were kindly gifted by Professor Xianwei Wang (Xinxiang Medical University, China). The cells were maintained in RPMI1640 culture medium (Gibco, USA) supplemented with 10% fetal bovine serum (Gibco), penicillin (100 IU/mL), and streptomycin (100 μg/mL) under 5% CO_2 and 37 °C conditions. Passages of 3–6 HUVECs were used in the present experiment. To evaluate the effects of high glucose on cell oxidative stress and ER stress, cells were maintained in normal (5.6 mmol/L) or high glucose (30 mmol/L) medium. AMG487 (1 μM) was applied to determine the roles of CXCR3. The dose was chosen based on a previous study [25]. To further discuss the effects of reactive oxygen species (ROS) generation on other physiological changes, the cells were treated with nicotinamide adenine dinucleotide phosphate (NADPH) oxidase inhibitor apocynin (10 μmol/L) [26].

2.8. Measurement of ROS, oxidative product malondialdehyde (MDA), and antioxidant enzyme activity (superoxide dismutase, SOD, and glutathione peroxidase, GSH-Px)

DHE, a ROS fluorescent probe, was used to detect the ROS level. Retinal cryosections or HUVECs were incubated with DHE (5 mM) at room temperature for 40 min in the dark. The fluorescence intensity was analyzed using the Image J software program. MDA content, SOD level, and GSH-Px activity were measured using commercial assay kits (Nanjing Jiancheng Bioengineering Institute, Nanjing, China).

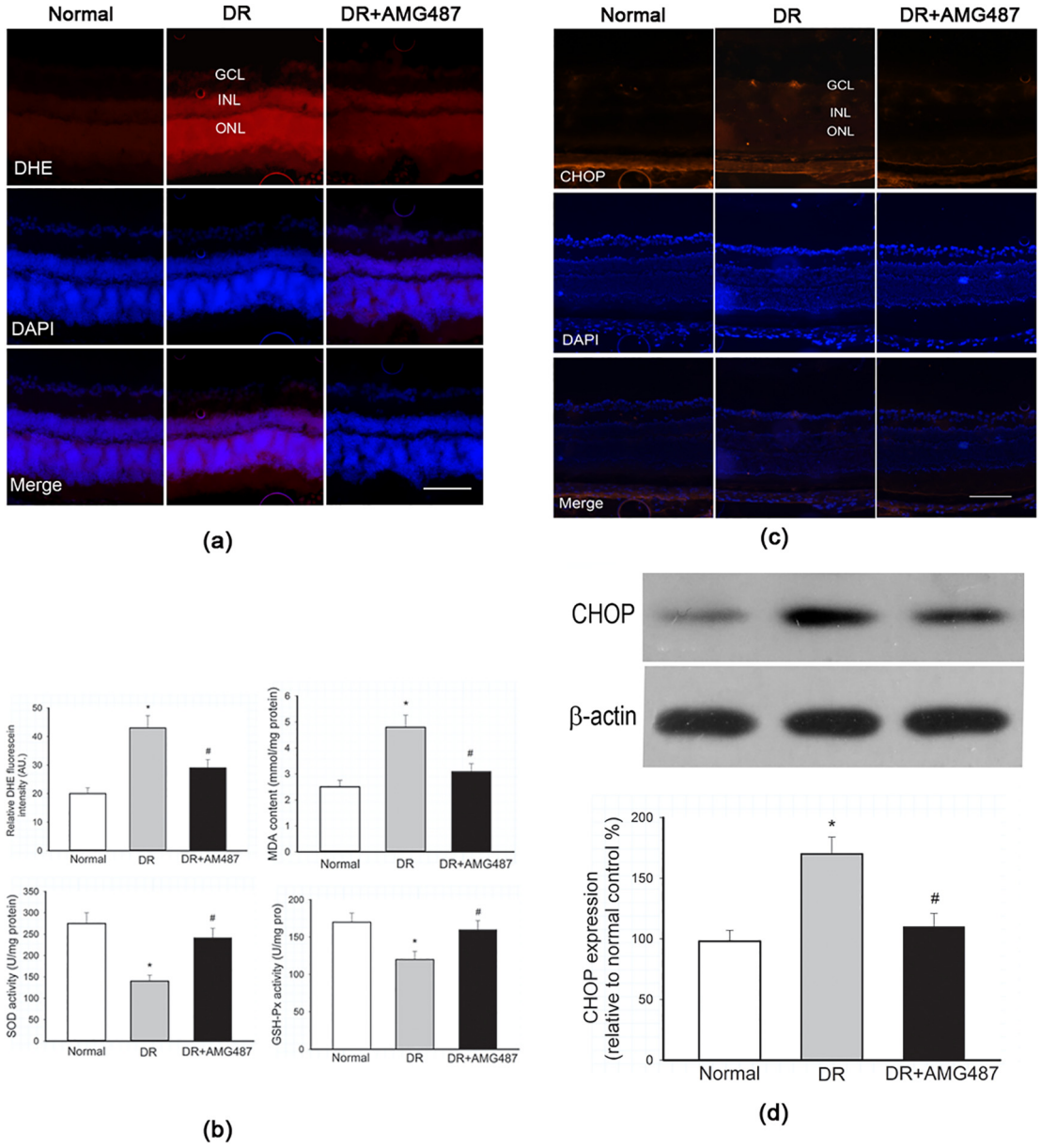

Fig. 5. Effects of AMG487 on ROS generation, MDA level, SOD and GSH-Px activities, and CHOP expression in DR retinas. (a) Representative images of DHE imaging; (b) Quantitative analysis of DHE intensity, MDA level, and SOD and GSH-Px activities; (c) Representative immunochemical staining images of CHOP; (d) Western blot analysis shows the increased CHOP expression in DR group were inhibited by the treatment of AMG487. GCL, ganglion cell layer; INL, inner nuclear layer; ONL, outer nuclear layer. Scale bar = 50 μm; *P < 0.05, compared with the normal control; #P < 0.05, compared with the DR group.

2.9. TUNEL assay

Cell apoptosis was detected using a one-step TUNEL apoptosis assay kit (Beyotime Biotech), according to the manufacturer's instructions. Apoptosis cells were counted under a fluorescence microscope.

2.10. Measurement of CXCL10 content by ELISA

HUVECs were seeded onto a 24-well plate. The cell culture supernate was collected and detected using an ELISA kit (Boster Biotechnology, China), according to the manufacturer's protocols.

2.11. Statistical analysis

All results were presented as mean ± SEM. Data were statistically analyzed using SigmaStat 3.5 (Systat software, Inc., SanJose, CA, USA). The differences in means among the groups were compared using one-way analysis of variance (Tukey's test or Kruskal–Wallis test were used as post-hoc tests) or Student's *t*-test. Differences were considered statistically significant at P values < 0.05.

3. Results

3.1. General description

Blood glucose was maintained at high levels (maximum level 33 mmol/L) in diabetic groups treated with and without AMG487 after the injection of STZ compared with the normal control group (Fig. 1a). Among the three groups of animals, body weight increased rapidly during the first 3 weeks. Then, the normal control group experienced slow growth, and the other two groups showed decreasing trends in bodyweight (Fig. 1a). The STZ-induced experimental diabetic mouse

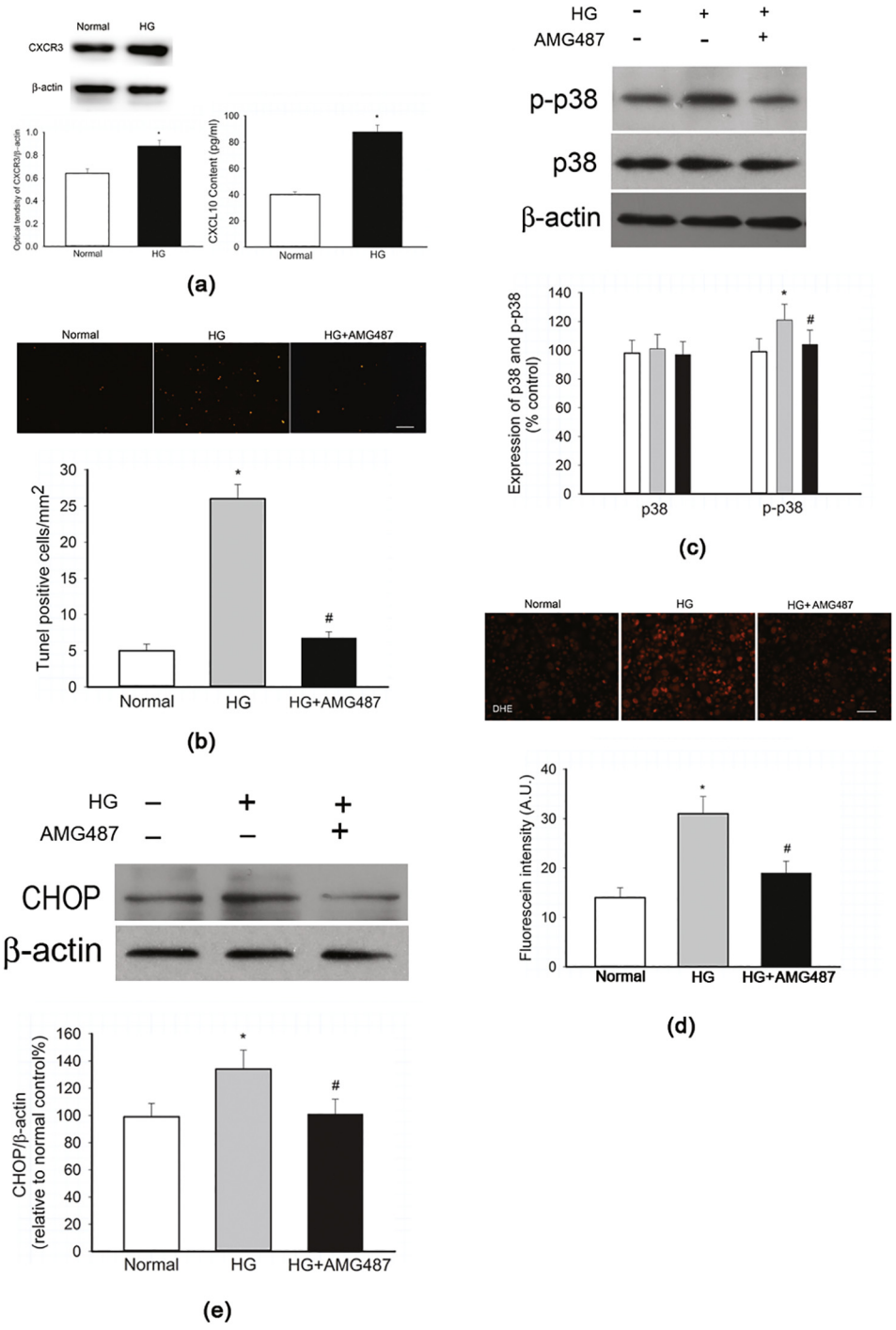

Fig. 6. AMG487 relieves high glucose-induced HUVEC cells apoptosis via the inhibition of p38, ROS, and CHOP pathway. (a) High glucose condition increased CXCR3 expression and CXCL10 release; (b) AMG487 decreased high glucose-induced cell apoptosis; (c) High glucose-induced p-p38 activation was inhibited by AMG487, (white column □) normal, (grey column ▒) high glucose, (black column ■) High glucose +AMG487; (d) High glucose-induced ROS generation was inhibited by AMG487; (e) High glucose-induced CHOP increase was inhibited by AMG487; Scale bar = 100 μm, $n = 5$, *P < 0.05, compared with normal control; #P < 0.05, compared with high glucose group.

model may present different diabetes types. Usually, small doses of STZ injected multiple times generate a type 1 diabetic animal model, which is involved in the autoimmune response process. To clarify the type of diabetes that was induced by the injection manner used in the present study (i.e., 75 mg/kg STZ i.p., on alternate days, three times), the blood insulin autoantibody (IAA) level and the pancreatic islet tissue slice were examined. The serum IAA level was measured with an ELISA kit in the 8th week following STZ injection. The IAA in the diabetic mice was significantly higher than that of the normal control group mice (Fig. 1c). Histology observation showed that the pancreatic islets in the diabetic mice were smaller and had fewer cell numbers than the normal group (Fig. 1d). Therefore, an experimental type 1 diabetic mouse model was produced in the present study. To determine whether the CXCR3 signaling was implicated in the process of DR, immunohistochemical staining and western blot analysis were performed. The results showed that CXCR3 expression was significantly upregulated at the end of the 8th week after STZ injection (Fig. 1e and f).

3.2. Ultrastructures of retinal capillary endothelial cell and ganglion cell observed under a transmission electron microscope

In the retinas of the diabetic group, the basement membrane of the capillary endothelial cell was thicker and the cytoplasm protruded to the lumen (Fig. 2 upper); for the retinal ganglion cells (Fig. 2 bottom), swelling and vacuolization were found in the cytoplasm, and the nuclear membranes were wrinkled. These changes were not seen in the

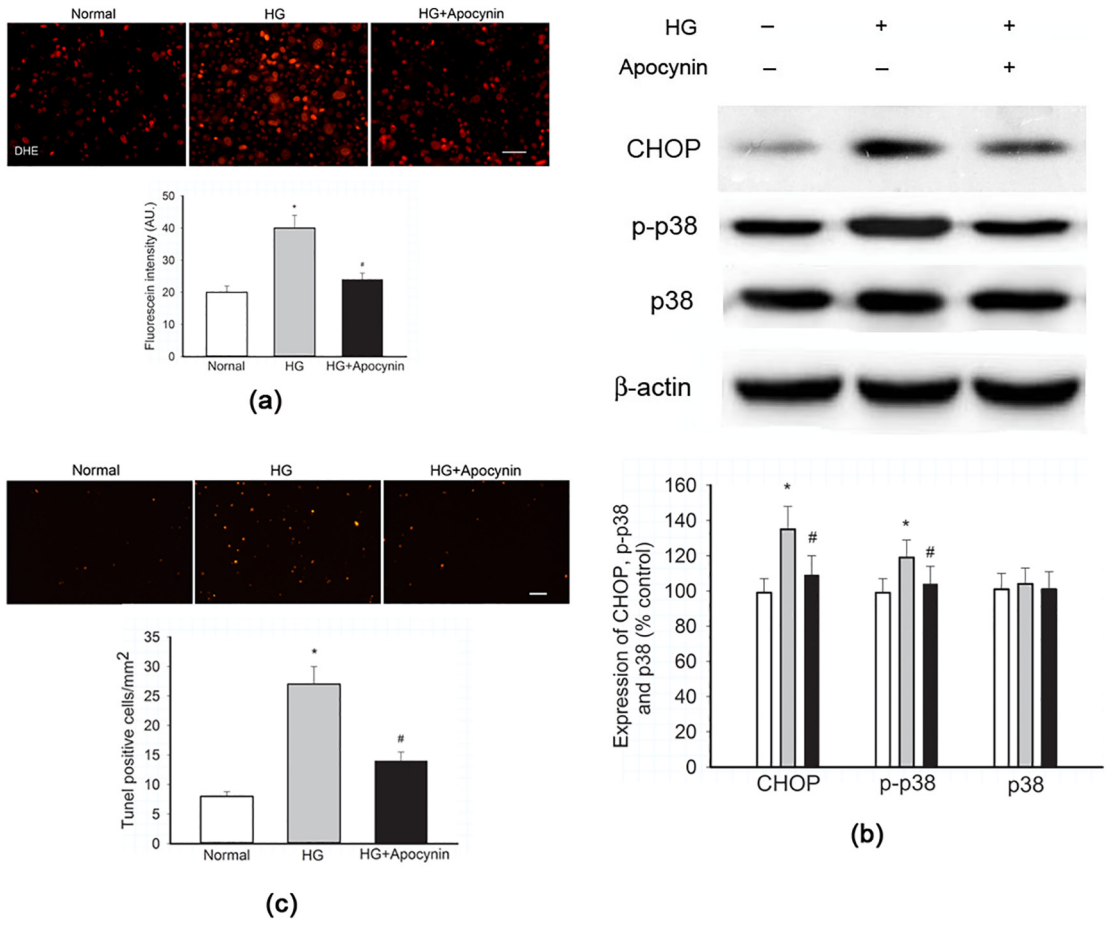

Fig. 7. Effects of ROS inhibition on p-p38, CHOP expression, and cell apoptosis. (a) DHE fluorescein intensity indicates the ROS generation; (b) Western blot analysis on the expression of CHOP, p-p38, and p38. (white column □) normal, (grey column ■) High glucose, (black column ■) High glucose + Apocynin; (c) TUNEL assay to determine the cell apoptosis. Scale bar = 100 μm, $n = 5$, *P < 0.05, compared with normal control; #P < 0.05, compared with the high glucose group.

retinal samples from the normal control group or the DR + AMG487 group. Thus, the diabetes-induced abnormal changes in the capillary and retinal ganglion cell can be prevented by AMG487 application.

3.3. Inhibition of CXCR3 decreased PDGFR-β and occludin loss in the diabetic retina

Pericyte is a critical factor for the maintenance of the integrity of blood vessel endothelium/BRB. The loss of pericytes may result in the breakdown of BRB in the diabetic retina. The role of CXCR3 for the integrity of BRB in diabetic mice was evaluated using western blot analysis for PDGFR-β expression. PDGFR-β, a pericyte marker, showed decreased expression in the diabetic retinas. However, the treatment of AMG487 prevented the reduction of the PDGFR-β expression in diabetic retinas (Fig. 3a). Occludin is a critical transmembrane protein, which belongs to the tight junction proteins member and forms the permeability barrier. In STZ-induced diabetic mouse model, Tight junction proteins could be reduced during the early few weeks after STZ injection [27]. Western blot analysis showed that occludin expression were decreased in diabetic retinas; however, the application of AMG487 prevented the reduction of occludin content (Fig. 3b).

3.4. AMG487 reduced the residual albumin content in the diabetic retinas

Under physiology conditions, the BRB is intact and mouse albumin is confined by the vascular endothelium. When BRB is broken down, the albumin might leak out into the retinal tissue. To evaluate the integrity of the BRB, the extravasation of albumin from the retinal vessels was examined after washing out the blood cells and proteins by cardiac perfusion. Retinal cross section immunostaining and western blot examinations showed that the extravasation of albumin was significantly increased in diabetic retinas. Diabetic mice treated with AMG487 displayed an obvious reduction of retinal extravasation of albumin (Fig. 4). Thus, the BRB that was broken down in diabetic mice could be prevented by AMG487 treatment.

3.5. AMG487 mitigated the oxidative stress and endoplasmic reticulum stress in the DR retina

Oxidative damage and ER stress are important pathological processes during the early stages of DR. To evaluate the effect of AMG487 on oxidative stress and ER stress in the STZ-induced diabetic mouse model, ROS level, lipid peroxidative product MDA content, antioxidant enzyme activity (SOD and GSH-Px), and the ER stress marker CHOP expression were measured. ROS fluorescent (red) probe-DHE may permeate into the cells and become oxidized by the intracellular ROS. The ROS fluorescence content in the diabetic retina was higher in the STZ-induced diabetic mice than in the normal control group. However, diabetic animals treated with AMG487 had significantly lower ROS fluorescence content (Fig. 5a). As shown in Fig. 5b, the MDA content in the DR group increased, and the SOD and GSH-Px activities decreased significantly. For the DR animals, the increase of MDA content, and decreae of SOD and GSH-Px activities were significantly mitigated by the AMG487 treatment (Fig. 5b). In addition, the ER stress marker CHOP was detected using immunostaining and western blot analysis. The results indicated that CHOP expression significantly increased in

the DR group, whereas this increase was inhibited after AGM487 treatment (Fig. 5c and d). Therefore, DR-induced retinal oxidative stress and ER stress can be mitigated by the application of CXCR3 antagonist AMG487.

3.6. AMG487 attenuated the HUVEC cell damage induced by high glucose via the CXCR3/p38/ROS pathway

To evaluate the effects of high glucose on endothelial cells, a HUVEC cell apoptosis model was established. CXCR3 expression, CXCL10 content, p38 activation, ROS generation, ER stress marker CHOP, and cell apoptosis were examined. After the cells were treated with high glucose for 72 h, CXCR3 expression and CXCL10 content increased significantly (Fig. 6a). Additionally, the apoptotic cells, p-p38 expression, ROS generation, and CHOP expression increased (Fig. 6b–e). The high glucose-induced changes could be mitigated by AMG487 application; therefore, the blocking of CXCR3 exerted protective roles against high glucose-induced cell death via the inhibition of p-p38, CHOP, and ROS.

3.7. Inhibition of ROS generation decreased cell apoptosis and p-p38 and CHOP expression

To further determine the effects of ROS on the high glucose-induced cell stress, the NADPH oxidase inhibitor apocynin was applied to the culture medium. The results showed that the application of apocynin decreased the high glucose-induced p-p38 expression, CHOP expression, and cell apoptosis (Fig. 7a–c). Therefore, the inhibition of ROS generation may induce negative feedback effects on p-p38 expression and mitigate the ER stress level, and further protect cells against apoptosis induced by high glucose.

4. Discussion

DR is the major cause of progressive visual impairment and blindness among the global adult population. Although the pathogenesis of DR is very complex, it has been widely recognized that oxidative stress and inflammatory-induced BRB dysfunction are the earliest and most significant pathological changes in DR. The present study revealed that the application of CXCR3 antagonist AMG487 played a role in antioxidative damage and prevention of BRB injury in the STZ-induced type 1 diabetic mouse model. The in vitro experiment revealed that high glucose in cultured HUVEC cells might increase CXCR3 expression and CXCL10 release. AMG487 can protect HUVEC cells against oxidative stress and ER stress-induced apoptosis under high glucose conditions.

Chemokine is a family of small chemotactic cytokines and is generated locally in inflammatory or damaged tissues. CXCR3 belongs to the chemokine CXC subclass, and is the receptor of CXCL9, CXCL10, and CXCL11. CXCR3 expression has been found in endothelial cells, microglia, neuron, and podocytes [12–15]. In the nervous system, CXCL10 and its receptor CXCR3 have been implicated in many disease models, such as neurodegeneration in the entorhinal cortex lesion model [16], NMDA-induced neuron death in the organotypic hippocampal slice culture model [14], the high intraocular pressure mouse model, and the optic nerve crush injury model [17,18]. In vascular endothelial cells, chemokine and its receptor play an important role in vascular inflammation. CXCR3 activation in endothelial cells not only limits angiogenesis, but also compromises vessel integrity to induce regression [12,13,28]. Usually, DR is the primary cause of vision impairment in the world. Approximately 1% of global blindness develops from diabetic patients according to the survey by the World Health Organization. Both type 1 and type 2 diabetes may induce vascular damage, although type 1 diabetes sufferers are more susceptible to DR. An epidemiological study stated that 71% of type 1 and 47% of type 2 diabetic patients have DR [29]. In the STZ-induced diabetic mouse model, the type classification is related to the dose and frequency of STZ injection [30]. It is generally considered that a larger STZ dose will induce explosive diabetes for greater toxicity; however, multiple injections of a small STZ dose could induce gradual minor damage to the pancreatic beta cells and then develop to type 1 diabetes after the autoimmune response becomes involved. In the present study, the results of the blood insulin autoantibody assay and pancreatic slice observation showed that the autoimmune response was produced in the animals after STZ injection; therefore, this is a type 1 diabetic mouse model.

Experiments have shown that CXCR3 signaling is implicated in retinal oxidative stress and inflammatory response in glaucoma mouse models [17,31]. The present study demonstrated that CXCR3 expression was upregulated during the early stage DR animals. BRB disruption is the early and core element in the retinal dysfunction of DR patients. Microangiopathy mainly includes dysfunction of the tight junction integrity, loss of pericytes and endothelial cells, hyperglycemia-induced oxidative stress, and inflammatory changes. The BRB is formed by tight junctions of three cellular types. These are retinal capillary endothelial cells that are covered with pericytes and muller cells. Tight junctions are comprised of occludin, claudins, and zonula occluden proteins [32]. When BRB is disrupted by ischemia or hyperglycemia, the levels of these tight junction proteins may decrease [22,23,27]. Evidence from previous studies has suggested that the death of retinal pericytes and endothelial cells appeared during the early stage of DR (usually called non-proliferative DR) [33–36]. PDGFR-β as a marker of vascular pericyte has been demonstrated in the brain and retina in a mouse model [37,38]. The present study showed that PDGFR-β and occludin expression were significantly decreased in DR retinas. However, the application of AMG487 stopped these reductions. The mechanism in the connection of CXCR3 and pericyte is still not clear. CXCR3 inhibition in the endothelial cells that protects pericytes and BRB in DR animals is probable. Further studies are required to clarify the direct mechanism. The leaking albumin from the capillaries into the retina was also evaluated and the results were consistent with the disruption of the integrity of BRB. Therefore, AMG487 can prevent BRB dysfunction during the early stage of DR.

Hyperglycemia-induced oxidative stress is also a critical pathway during the pathological process of DR. When the body suffers from harmful stimulus, for instance hyperglycemia, ROS generation is abundant and the endogenous antioxidant system (SOD and GSH-Px) cannot scavenge them in a timely fashion. Then, oxidative damage will occur. The retina contains more polyunsaturated fatty acids and oxygen uptake relative to other tissues; therefore, it is more vulnerable to oxidative damage [39]. In the current DR mouse model after STZ injection for 8 weeks, ROS generation and MDA level increased significantly, whereas SOD and GSH-Px activities decreased. Therefore, the retinas in the DR group suffered from oxidative damage, which was in accordance with previous experiments [5,22,23,40]. The hyperglycemia-induced retinal oxidative stress may be ameliorated by AMG487 application. As CXCR3 antagonists, AMG487 is the only small molecule that has entered clinical trials. Previous studies demonstrated that AMG487 possessed efficacy in bleomycin-induced lung inflammation in mice [21], in pathology of chronic itch [20], and in optic nerve acute injury-induced retinal dysfunction and cell loss [18]. The blocking of CXCR3 may protect intraocular hypertension-induced retina injury via the reduction of oxidative stress and ER stress [17]. Furthermore, the CXCL10/CXCR3 axis plays a critical role in the recruitment of leukocytes and retinal injury in traumatic optic neuropathy. Deleting CXCR3 or treatment with CXCR3 antagonist AMG487 significantly prevented retinal ganglion cell loss and dysfunction from optic nerve injury [18]. AMG487, as a CXCR3 inhibitor, may decrease leukostasis and leukocyte infiltration in many diseases including DR; therefore, the ROS increasing formation induced by the leukocyte infiltration may be inhibited by AMG487 application during the diabetic condition. The antioxidase activity could decrease with the continuous increase in ROS levels. When the ROS was attenuated, the antioxidase could be protected, just as the present study suggestion that the decreased SOD and

GSH-Px activities in DR animals were significantly mitigated by the AMG487 application.

The chemokine receptor CXCR3 is expressed in microglia/monocyte, endothelial cells, and natural killer cells. The CXCR3 axis is involved in several diseases, such as rheumatoid arthritis, multiple sclerosis, atherosclerosis, and Alzheimer's disease [41,42]. To illustrate the role of the CXCL10/CXCR3 axis in endothelial cells suffering from high glucose, we cultured HUVEC cells under high glucose conditions. High glucose led to a significant increase in CXCR3 expression and CXCL10 release. Furthermore, the apoptotic cells, CHOP expression, ROS generation, and p-p38 level also increased. These high glucose-induced changes were reduced by the application of AMG487. Therefore, in the unicellular environment, CXCL1O/CXCR3 expression might be enhanced together with the upregulation of ROS generation under a high glucose condition, and blockade of CXCR3 was helpful for protecting cell damage against oxidative stress. This process was involved in the activation of p38 and the upregulation of CHOP, an ER stress marker. Oxidative stress and ER stress always exert interactional effects in many situations [43–45]. p38 is a mitogen-activated protein kinase (MAPK) singling pathway and can be activated by various inflammatory cytokines and ROS [46]. Likewise, NADPH oxidase and ROS generation are under the regulation of p38 MAPK [47,48]. It has been suggested that the activation of p38 is related to the diabetes-induced pericyte and endothelial cell death [49]. Therefore, in the present study, CXCR3 activation and/or high expression, which might promote p38 activation, might be via paracellular secretion or autocrine in HUVEC cells under high glucose conditions.

In summary, the present study demonstrated that CXCR3 blockade played a protective role in diabetes-induced BRB disruption via anti-oxidative stress and inhibition of ER stress. However, there are some limitations to the study. First, many new small molecule CXCR3 antagonists have emerged recently; however, we only chose to study the antagonist AMG487 in the present study because it was the only one that had been entered into clinical trials. Second, blocking of CXCR3 with gene knockout maybe have different views. Finally, results regarding intravitreal injection of AMG487 should be obtained. Further studies are required to determine the exact role of the CXCR3 antagonist on DR. In conclusion, the inhibition of CXCR3 by AMG487 exerted protective actions on DR-induced BRB. Thus, this could be a promising treatment strategy for the early stages of DR.

Conflict of interest statement

The authors declare that no commercial and associative interests that represent conflicted interests in connection with the work submitted.

Author contribution to study

W, HG: project administration, writing.
L, JM; Z, PY; W, SW: experiments, methodology.
Z, L; W, DD; C, ML: resources, software.
J, AL; L, YZ: supervision.
W, J: funding acquisition, conceptualization, data curation, original draft.

Acknowledgment

This work was funded by the National Natural Science Foundation of China (grant No. 31300884, 81803573).

Disclosure

The authors declare no commercial and associative interests that represent conflicted interests in connection with the work submitted.

References

[1] J. Tang, T.S. Kern, Inflammation in diabetic retinopathy, Prog. Retin. Eye Res. 30 (2011) 343–358.
[2] T.S. Kern, Contributions of inflammatory processes to the development of the early stages of diabetic retinopathy, Exp. Diabetes Res. 2007 (2007) 95103.
[3] Z. Ghanian, S. Mehrvar, N. Jamali, N. Sheibani, M. Ranji, Time-lapse microscopy of oxidative stress demonstrates metabolic sensitivity of retinal pericytes under high glucose condition, J. Biophotonics 11 (9) (2018) e201700289.
[4] A. Mazzeo, A.I. Arroba, E. Beltramo, A.M. Valverde, M. Porta, Somatostatin protects human retinal pericytes from inflammation mediated by microglia, Exp. Eye Res. 164 (2017) 46–54.
[5] R.S. Eshaq, W.S. Wright, N.R. Harris, Oxygen delivery, consumption, and conversion to reactive oxygen species in experimental models of diabetic retinopathy, Redox Biol. 2 (2014) 661–666.
[6] K. Trudeau, A.J. Molina, W. Guo, S. Roy, High glucose disrupts mitochondrial morphology in retinal endothelial cells: implications for diabetic retinopathy, Am. J. Pathol. 177 (2010) 447–455.
[7] Y.R. Chung, J.A. Choi, J.Y. Koh, Y.H. Yoon, Ursodeoxycholic acid attenuates endoplasmic reticulum stress-related retinal pericyte loss in streptozotocin-induced diabetic mice, J. Diabetes Res. 2017 (2017) 1763292.
[8] T.S. Kern, Contributions of inflammatory processes to the development of the early stages of diabetic retinopathy, Exp. Diabetes Res. 2007 (2007) 95103.
[9] N.S. Harhaj, E.A. Felinski, E.B. Wolpert, J.M. Sundstrom, T.W. Gardner, D.A. Antonetti, VEGF activation of protein kinase C stimulates occludin phosphorylation and contributes to endothelial permeability, Invest. Ophthalmol. Vis. Sci. 47 (2006) 5106–5115.
[10] A.M. Joussen, T. Murata, A. Tsujikawa, B. Kirchhof, S.E. Bursell, A.P. Adamis, Leukocyte-mediated endothelial cell injury and death in the diabetic retina, Am. J. Pathol. 158 (2001) 147–152.
[11] S. Lacotte, S. Brun, S. Muller, H. Dumortier, CXCR3, inflammation, and autoimmune diseases, Ann. N. Y. Acad. Sci. 1173 (2009) 310–317.
[12] X. Zhu, Y. Zou, B. Wang, J. Zhu, Y. Chen, L. Wang, J. Li, X. Deng, Blockade of CXC chemokine receptor 3 on endothelial cells protects against sepsis-induced acute lung injury, J. Surg. Res. 204 (2016) 288–296.
[13] R.J. Bodnar, M.E. Rodgers, W.C. Chen, A. Wells, Pericyte regulation of vascular remodeling through the CXC receptor 3, Arterioscler. Thromb. Vasc. Biol. 33 (2013) 2818–2829.
[14] H.R. van Weering, H.W. Boddeke, J. Vinet, N. Brouwer, A.H. de Haas, N. van Rooijen, A.R. Thomsen, K.P. Biber, CXCL10/CXCR3 signaling in glia cells differentially affects NMDA-induced cell death in CA and DG neurons of the mouse hippocampus, Hippocampus 21 (2011) 220–232.
[15] E.K. de Jong, A.H. de Haas, N. Brouwer, H.R. van Weering, M. Hensens, I. Bechmann, P. Pratley, E. Wesseling, H.W. Boddeke, K. Biber, Expression of CXCL4 in microglia in vitro and in vivo and its possible signaling through CXCR3, J. Neurochem. 105 (2008) 1726–1736.
[16] A. Rappert, I. Bechmann, T. Pivneva, J. Mahlo, K. Biber, C. Nolte, A.D. Kovac, C. Gerard, H.W. Boddeke, R. Nitsch, H. Kettenmann, CXCR3-dependent microglial recruitment is essential for dendrite loss after brain lesion, J. Neurosci. 24 (2004) 8500–8509.
[17] Y. Ha, H. Liu, Z. Xu, H. Yokota, S.P. Narayanan, T. Lemtalsi, S.B. Smith, R.W. Caldwell, R.B. Caldwell, W. Zhang, Endoplasmic reticulum stress-regulated CXCR3 pathway mediates inflammation and neuronal injury in acute glaucoma, Cell Death Dis. 6 (2015) e1900.
[18] Y. Ha, H. Liu, S. Zhu, P. Yi, W. Liu, J. Nathanson, R. Kayed, B. Loucas, J. Sun, L.J. Frishman, M. Motamedi, W. Zhang, Critical role of the CXCL10/C-X-C chemokine receptor 3 axis in promoting leukocyte recruitment and neuronal injury during traumatic optic neuropathy induced by optic nerve crush, Am. J. Pathol. 187 (2017) 352–365.
[19] E.A. Abu, S. Struyf, D. Kangave, K. Geboes, J. Van Damme, Chemokines in proliferative diabetic retinopathy and proliferative vitreoretinopathy, Eur. Cytokine Netw. 17 (2006) 155–165.
[20] L. Qu, K. Fu, J. Yang, S.G. Shimada, R.H. LaMotte, CXCR3 chemokine receptor signaling mediates itch in experimental allergic contact dermatitis, Pain 156 (2015) 1737–1746.
[21] M. Johnson, A.R. Li, J. Liu, Z. Fu, L. Zhu, S. Miao, X. Wang, Q. Xu, A. Huang, A. Marcus, F. Xu, K. Ebsworth, E. Sablan, J. Danao, J. Kumer, D. Dairaghi, C. Lawrence, T. Sullivan, G. Tonn, T. Schall, T. Collins, J. Medina, Discovery and optimization of a series of quinazolinone-derived antagonists of CXCR3, Bioorg. Med. Chem. Lett. 17 (2007) 3339–3343.
[22] J. Wang, S. Wang, M. Li, D. Wu, F. Liu, R. Yang, S. Ji, A. Ji, Y. Li, The Neuropilin-1 inhibitor, ATWLPPR peptide, prevents experimental diabetes-induced retinal injury by preserving vascular integrity and decreasing oxidative stress, PLoS One 10 (2015) e142571.
[23] M. Rojas, W. Zhang, Z. Xu, T. Lemtalsi, P. Chandler, H.A. Toque, R.W. Caldwell, R.B. Caldwell, Requirement of NOX2 expression in both retina and bone marrow for diabetes-induced retinal vascular injury, PLoS One 8 (2013) e84357.
[24] B. Cambien, B.F. Karimdjee, P. Richard-Fiardo, H. Bziouech, R. Barthel, M.A. Millet, V. Martini, D. Birnbaum, J.Y. Scoazec, J. Abello, S.T. Al, M.G. Johnson, T.J. Sullivan, J.C. Medina, T.L. Collins, A. Schmid-Alliana, H. Schmid-Antomarchi, Organ-specific inhibition of metastatic colon carcinoma by CXCR3 antagonism, Br. J. Cancer 100 (2009) 1755–1764.
[25] T.C. Walser, S. Rifat, X. Ma, N. Kundu, C. Ward, O. Goloubeva, M.G. Johnson, J.C. Medina, T.L. Collins, A.M. Fulton, Antagonism of CXCR3 inhibits lung metastasis in a murine model of metastatic breast cancer, Cancer Res. 66 (2006)

7701–7707.
[26] A. Taye, A.H. Saad, A.H. Kumar, H. Morawietz, Effect of apocynin on NADPH oxidase-mediated oxidative stress-LOX-1-eNOS pathway in human endothelial cells exposed to high glucose, Eur. J. Pharmacol. 627 (2010) 42–48.
[27] D.A. Antonetti, A.J. Barber, S. Khin, E. Lieth, J.M. Tarbell, T.W. Gardner, Vascular permeability in experimental diabetes is associated with reduced endothelial occludin content: vascular endothelial growth factor decreases occludin in retinal endothelial cells. Penn State Retina Research Group, Diabetes 47 (1998) 1953–1959.
[28] L. Lasagni, M. Francalanci, F. Annunziato, E. Lazzeri, S. Giannini, L. Cosmi, C. Sagrinati, B. Mazzinghi, C. Orlando, E. Maggi, F. Marra, S. Romagnani, M. Serio, P. Romagnani, An alternatively spliced variant of CXCR3 mediates the inhibition of endothelial cell growth induced by IP-10, Mig, and I-TAC, and acts as functional receptor for platelet factor 4, J. Exp. Med. 197 (2003) 1537–1549.
[29] C. Zhang, H. Wang, J. Nie, F. Wang, Protective factors in diabetic retinopathy: focus on blood-retinal barrier, Discov. Med. 18 (2014) 105–112.
[30] N. Sun, G. Yang, H. Zhao, H.F. Savelkoul, L. An, Multidose streptozotocin induction of diabetes in BALB/c mice induces a dominant oxidative macrophage and a conversion of TH1 to TH2 phenotypes during disease progression, Mediat. Inflamm. 2005 (2005) 202–209.
[31] A. Denoyer, D. Godefroy, I. Celerier, J. Frugier, J. Degardin, J.K. Harrison, F. Brignole-Baudouin, S. Picaud, F. Baleux, J.A. Sahel, W. Rostene, C. Baudouin, CXCR3 antagonism of SDF-1(5-67) restores trabecular function and prevents retinal neurodegeneration in a rat model of ocular hypertension, PLoS One 7 (2012) e37873.
[32] J. Cunha-Vaz, R. Bernardes, C. Lobo, Blood-retinal barrier, Eur. J. Ophthalmol. 21 (Suppl. 6) (2011) S3–S9.
[33] S. Suarez, G.W. McCollum, A. Jayagopal, J.S. Penn, High glucose-induced retinal pericyte apoptosis depends on association of GAPDH and Siah1, J. Biol. Chem. 290 (2015) 28311–28320.
[34] E. Beltramo, M. Porta, Pericyte loss in diabetic retinopathy: mechanisms and consequences, Curr. Med. Chem. 20 (2013) 3218–3225.
[35] D.J. Feenstra, E.C. Yego, S. Mohr, Modes of retinal cell death in diabetic retinopathy, J. Clin. Exp. Ophthalmol 4 (2013) 298.
[36] M.M. Nentwich, M.W. Ulbig, Diabetic retinopathy - ocular complications of diabetes mellitus, World J. Diabetes 6 (2015) 489–499.
[37] P. Lindahl, B.R. Johansson, P. Leveen, C. Betsholtz, Pericyte loss and microaneurysm formation in PDGF-B-deficient mice, Science 277 (1997) 242–245.
[38] M. Hellstrom, M. Kalen, P. Lindahl, A. Abramsson, C. Betsholtz, Role of PDGF-B and PDGFR-beta in recruitment of vascular smooth muscle cells and pericytes during embryonic blood vessel formation in the mouse, Development 126 (1999) 3047–3055.
[39] R.E. Anderson, L.M. Rapp, R.D. Wiegand, Lipid peroxidation and retinal degeneration, Curr. Eye Res. 3 (1984) 223–227.
[40] H. Liu, J. Tang, C.A. Lee, T.S. Kern, Metanx and early stages of diabetic retinopathy, Invest. Ophthalmol. Vis. Sci. 56 (2015) 647–653.
[41] D. Galimberti, N. Schoonenboom, P. Scheltens, C. Fenoglio, F. Bouwman, E. Venturelli, I. Guidi, M.A. Blankenstein, N. Bresolin, E. Scarpini, Intrathecal chemokine synthesis in mild cognitive impairment and Alzheimer disease, Arch. Neurol. 63 (2006) 538–543.
[42] K.E. Balashov, J.B. Rottman, H.L. Weiner, W.W. Hancock, CCR5(+) and CXCR3(+) T cells are increased in multiple sclerosis and their ligands MIP-1alpha and IP-10 are expressed in demyelinating brain lesions, Proc. Natl. Acad. Sci. U. S. A. 96 (1999) 6873–6878.
[43] A. Higa, E. Chevet, Redox signaling loops in the unfolded protein response, Cell. Signal. 24 (2012) 1548–1555.
[44] J.D. Malhotra, R.J. Kaufman, The endoplasmic reticulum and the unfolded protein response, Semin. Cell Dev. Biol. 18 (2007) 716–731.
[45] B.H. Abuaita, K.M. Burkholder, B.R. Boles, M.X. O'Riordan, The endoplasmic reticulum stress sensor inositol-requiring enzyme 1alpha augments bacterial killing through sustained oxidant production, MBIO 6 (2015) e705.
[46] J.M. Kyriakis, J. Avruch, Mammalian MAPK signal transduction pathways activated by stress and inflammation: a 10-year update, Physiol. Rev. 92 (2012) 689–737.
[47] W. Bao, D.J. Behm, S.S. Nerurkar, Z. Ao, R. Bentley, R.C. Mirabile, D.G. Johns, T.N. Woods, C.P. Doe, R.W. Coatney, J.F. Ohlstein, S.A. Douglas, R.N. Willette, T.L. Yue, Effects of p38 MAPK inhibitor on angiotensin II-dependent hypertension, organ damage, and superoxide anion production, J. Cardiovasc. Pharmacol. 49 (2007) 362–368.
[48] B.K. Yoo, J.W. Choi, C.Y. Shin, S.J. Jeon, S.J. Park, J.H. Cheong, S.Y. Han, J.R. Ryu, M.R. Song, K.H. Ko, Activation of p38 MAPK induced peroxynitrite generation in LPS plus IFN-gamma-stimulated rat primary astrocytes via activation of iNOS and NADPH oxidase, Neurochem. Int. 52 (2008) 1188–1197.
[49] Y. Du, J. Tang, G. Li, L. Berti-Mattera, C.A. Lee, D. Bartkowski, D. Gale, J. Monahan, M.R. Niesman, G. Alton, T.S. Kern, Effects of p38 MAPK inhibition on early stages of diabetic retinopathy and sensory nerve function, Invest. Ophthalmol. Vis. Sci. 51 (2010) 2158–2164.